Chaos-Assisted Directional Light Emission from Microcavity Lasers

Susumu Shinohara,[1] Takahisa Harayama,[2] Takehiro Fukushima,[3] Martina Hentschel,[1] Takahiko Sasaki,[4] and Evgenii E. Narimanov[5]

[1]*Max-Planck-Institut für Physik Komplexer Systeme, Nöthnitzer Straße 38, D-01187 Dresden, Germany*
[2]*NTT Communication Science Laboratories, NTT Corporation, 2-4 Hikaridai, Seika-cho, Soraku-gun, Kyoto 619-0237, Japan*
[3]*Department of Communication Engineering, Okayama Prefectural University, 111 Kuboki, Soja, Okayama 719-1197, Japan*
[4]*Center for Nano Materials and Technology, Japan Advanced Institute of Science and Technology, 1-1 Asahidai, Nomi, Ishikawa 923-1292, Japan*
[5]*Birck Nanotechnology Center, Department of Electrical and Computer Engineering, Purdue University, 1205 West State Street West Lafayette, Indiana 47907-2057, USA*

(Received 1 December 2009; published 21 April 2010)

We study the effect of dynamical tunneling on emission from ray-chaotic microcavities by introducing a suitably designed deformed disk cavity. We focus on its high quality factor modes strongly localized along a stable periodic ray orbit confined by total internal reflection. It is shown that dominant emission originates from the tunneling from the periodic ray orbit to chaotic ones; the latter eventually escape from the cavity refractively, resulting in directional emission that is unexpected from the geometry of the periodic orbit, but fully explained by unstable manifolds of chaotic ray dynamics. Experimentally performing selective excitation of those modes, we succeeded in observing the directional emission in good agreement with theoretical prediction. This provides decisive experimental evidence of dynamical tunneling in a ray-chaotic microcavity.

DOI: 10.1103/PhysRevLett.104.163902 PACS numbers: 42.55.Sa, 05.45.Mt, 42.55.Px, 42.60.Da

Dynamical billiards have served as a simple and generic model in studies of classical and quantum chaos. Whereas originally a dynamical billiard was introduced as an abstract model for studying the ergodic hypothesis [1], nowadays it has been realized as a physical system that confines microwaves, acoustics, electrons, and light [2]. As for billiards for light [3–5], or optical microcavities, the openness of a system intrinsic to light confinement necessitated the studies of decaying modes, or resonances of the Helmholtz equation, which had been less studied in the field of quantum chaos. Resonance characteristics such as quality factors and emission patterns have been intensively studied in terms of classical and quantum chaos theory [6]. These studies are also motivated by practical applications of optical microcavities. When they are applied for laser resonators, there is a demand that modes have both high quality factors and high emission directionality.

A high quality factor mode can be associated with a ray orbit confined by total internal reflection (TIR), whose representative example is the whispering-gallery (WG) modes of a disk cavity. It was demonstrated that the introduction of a slight asymmetric deformation to a disk shape enables the existence of a WG-like mode with emission directionality [3]. However, in general, such a mode is embedded in a variety of high quality factor modes that do not necessarily have similar emission directionality, implying that experimentally it is not easy to selectively excite only desired directional modes.

For a large deformation, ray dynamics inside the cavity becomes mostly chaotic, which causes degradation of quality factors. However, low-loss modes start to exhibit a universal emission pattern, which can be well explained by the unstable manifolds of an unstable periodic orbit close to the TIR condition [7]. The universal emission pattern can be highly directional by properly designing an unstable manifold structure [8]. Because low-loss modes, likely to be excited with a lasing medium, have a similar emission pattern, one can experimentally achieve directional emission without any settings for selective excitation. For those low-loss modes, relatively high quality factors are attributed to wave localization along TIR-confined unstable periodic orbits [8], which is, however, generally weaker than localization along a TIR-confined WG orbit or a TIR-confined stable periodic orbit.

In this Letter, introducing a novel largely deformed disk cavity, we study high quality factor modes with emission directionality made possible by a dynamical tunneling phenomenon [9,10]. The key point is mostly chaotic ray dynamics having a single dominant stable periodic orbit confined by TIR. The high quality factors come from strong localization of the modes along the TIR-confined stable periodic orbit. If one adopts a one-dimensional or integrable picture based, for instance, on the Gaussian-optic theory [11], one would expect extremely weak emission due to TIR for those modes. However, in reality, tunneling from the periodic orbit to neighboring chaotic orbits takes place, where the latter eventually escape out from the cavity refractively following unstable manifolds. Namely, light is emitted with the assistance of chaos. Fabricating laser diodes with this deformed disk shape

with an electrode contact patterned along the TIR-confined periodic orbit, we experimentally perform selective excitation of the high quality factor modes and demonstrate chaos-assisted directional emission in good agreement with theoretical prediction.

We first define the deformed disk cavity. In the polar coordinates, its boundary is defined by $r(\phi) = R(1 + a\cos 2\phi + b\cos 4\phi + c\cos 6\phi)$, where R is the size parameter and a, b, and c are deformation parameters fixed as $a = 0.1$, $b = 0.01$, and $c = 0.012$ [Fig. 1(a)]. Features of internal ray dynamics can be best described by using the Poincaré surface of section (SOS). The Poincaré SOS is a reduction of ray dynamics to a two-dimensional mapping describing successive bounces of a ray orbit. The variables of the mapping are a canonical conjugate pair called the Birkhoff coordinates, s and $\sin\theta$, where s is the arclength measured along the cavity boundary and $\sin\theta$ the tangential momentum of an incident ray [Fig. 1(a)]. We show the SOS of our cavity in Fig. 1(c), which reveals that ray dynamics is mostly chaotic, except for several islands of stability. Dominant islands are period-two islands at around $\sin\theta = 0$ and period-four islands at around $\sin\theta = 0.7$. Figure 1(b) shows a rectangular orbit corresponding to the period-four stable periodic points. This orbit is confined by TIR when the laser is made from GaAs/AlGaAs quantum-well structure (i.e., the effective refractive index $n = 3.3$). In Fig. 1(c), the critical line for TIR, $\sin\theta = 1/n$, is plotted by a dashed line, above which rays are reflected by TIR. The key feature of our cavity is that there exists only one dominant stable periodic

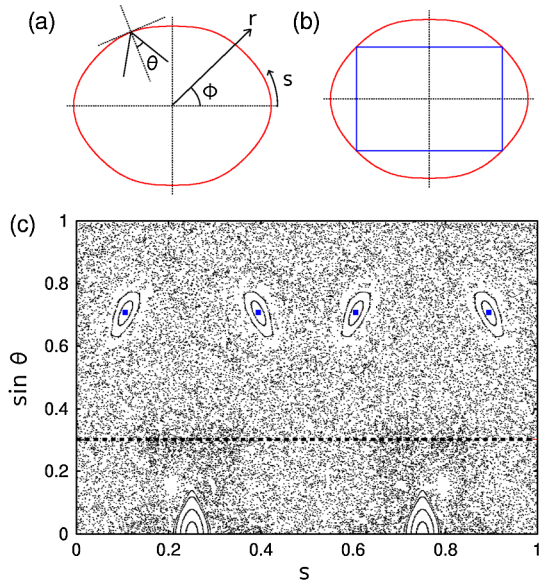

FIG. 1 (color online). (a) Geometry of the deformed disk cavity. (b) The rectangular ray orbit. (c) The upper half of the Poincaré surface of section for internal ray dynamics. The variable s is normalized by the total circumference. The four filled rectangles (■) plotted at $\sin\theta \approx 0.7$ correspond to the rectangular ray orbit. The critical line for total internal reflection, $\sin\theta = 1/3.3$, is plotted by a dashed line.

orbit above the critical line and it is surrounded by a chaotic sea extending into the non-TIR (i.e., leaky) region, $|\sin\theta| < 1/n$.

We are interested in resonant modes corresponding to the TIR-confined rectangular orbit. For those modes, there are two expected emission mechanisms. One is evanescent emission, which occurs at the four bouncing points of the rectangular orbit, yielding emission in the tangential direction to the cavity boundary, i.e., $\phi = 45°$, $135°$, $225°$, and $315°$. Another mechanism is due to dynamical tunneling [9–11]. An orbit on the period-four islands tunnels to a neighboring chaotic orbit and it eventually diffuses into the leaky region, yielding refractive light emission. In order to capture the effect of dynamical tunneling on emission patterns precisely, next we study wave functions of resonant modes.

Resonant modes can be obtained by solving a linear Helmholtz equation numerically [12]. We consider transverse electric (TE) polarization, in order to be consistent with our experiments described below. We systematically study resonant modes whose scaled wave number kR is around 50, where k is the free-space wave number. We checked that properties of resonant modes discussed here are essentially the same for a larger cavity (e.g., $kR = 100$).

Employing the Husimi projection of a wave function onto the SOS, we could classify resonant modes into three classes: rectangle-orbit modes, WG-type modes, and chaotic modes. Here we exclude highly lossy modes such as the one residing on the period-two islands in the leaky region. Rectangle-orbit modes are strongly localized on the period-four islands, while WG-type modes are strongly localized on the upper or lower verges of the SOS (i.e., $|\sin\theta| \lesssim 1$). Chaotic modes are mostly distributed in the chaotic sea, even largely spreading into the leaky region. The first two classes of modes have high quality factors $Q \approx 10^5$–10^6, as they are localized in the TIR regions, whereas typical chaotic modes have low quality factors $Q \approx 100$.

We plot in Fig. 2 the wave function of a rectangle-orbit mode, where the intensity outside the cavity is plotted in log scale in order to clearly see the emission pattern. Figure 2 reveals that light is emitted towards $\phi = \pm 90°$ on both sides of the cavity, i.e.,$\phi \approx 0°$ and $180°$. By careful inspection, one finds that light is emitted from four cavity boundary points corresponding to polar angles $\phi = \pm 4°$ and $\phi = 180 \pm 4°$. In the corresponding far-field pattern (to be presented in Fig. 5), two distinct peaks appear at $\phi = \pm 90°$ with a divergence angle $30°$. Moreover, in each peak, we observe the interference pattern of light beams emitted from both sides of the cavity, whose oscillation period is given by $\Delta\theta = 360°/kd$ with $d = 2R(1 + a + b + c)$ being the width of the cavity. We confirmed that emission patterns are almost similar for all rectangle-orbit modes. Although it appears counterintuitive that light is emitted from positions apart from the

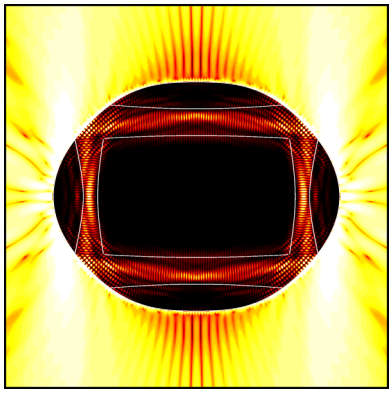

FIG. 2 (color online). Wave function for a rectangle-orbit mode with a wave number $\mathrm{Re}kR = 49.94$ and $\mathrm{Im}kR = -0.000\,12$. The intensity increases as the color changes from black to white. Outside the cavity, the intensity is plotted in log scale. The outline of the electrode contact window is indicated by white curves.

rectangular orbit, its mechanism can be explained by dynamical tunneling as we see next.

Figure 3 shows the log plot of the Husimi projection of the wave function shown in Fig. 2. Because the Husimi projection is symmetric with respect to the transformation $(s, \sin\theta) \mapsto (1 - s, -\sin\theta)$, only the upper half part is shown. The intensity is mostly concentrated around the period-four islands, but we can see some intensity also spread in the chaotic sea, which can be interpreted as the effect of dynamical tunneling. What determines the emission pattern is the intensity distribution in the leaky region. Around the critical line for TIR, we can observe two relatively high intensity spots at $s = 0.04$ and $s = 0.54$. It is these that are responsible for the emission towards $\phi = \pm 90°$.

It is explainable by ray dynamics why emission occurs at $s = 0.04$ and $s = 0.54$. In Fig. 3, we superimpose unstable

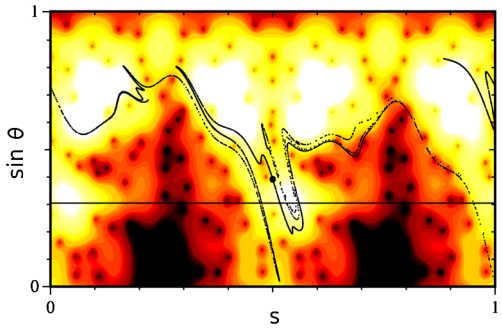

FIG. 3 (color online). The Husimi projection of the rectangle-orbit mode shown in Fig. 2. The intensity increases as the color changes from black to white. The intensity is plotted in log scale. The critical line for total internal reflection is plotted by a solid line. Unstable manifolds emanating from a period-three unstable periodic point at $(s, \sin\theta) = (0.5, 0.389\ldots)$, indicated by a filled circle, are plotted by a solid curve. The high intensity spots around the critical line at $s = 0.04$ and $s = 0.54$ correspond to emission towards $\phi = 90°$ and $\phi = -90°$, respectively.

manifolds of a period-three unstable periodic point onto the Husimi projection. This periodic point is located close to the critical line and thus its unstable manifolds govern a ray-dynamical flow around the critical line [7]. The structure of the unstable manifolds indicate that ray orbits are transported from the TIR region to the leaky region at around $s = 0.5$ (and $s = 0$ as well because of the 180° rotational symmetry of the cavity). This ray-dynamical argument also explains why emission patterns of the rectangle-orbit modes are almost similar.

Now we would like to examine whether the chaos-assisted light emission can be experimentally observed. We fabricated single-quantum-well laser diodes with the deformed disk cavities discussed above. The laser diodes are fabricated by applying a reactive-ion-etching technique to a graded-index separate-confinement-heterostructure single-quantum-well GaAs/AlGaAs structure that was grown by metal organic chemical vapor deposition. The lasing wavelength is around 850 nm. The cavity size R is set as 50 μm, yielding the scaled wave number $kR = 370$. In order to inject current only to rectangle-orbit modes, the electrode contact window was patterned along the rectangular orbit. Its outline is shown by white curves in Fig. 2. For current injection, an electrode metal is coated on the cavity top, which covers all over the top except for some margin of the cavity. The precise shape of the electrode metal is defined by $r < Mr(\phi)$ with the margin parameter $M(\leq 1)$. Because of an intervening SiO_2 insulation layer, the electrode metal only touches the GaAs contact layer through the contact window [5]. With this structure, we can selectively excite rectangle-orbit modes, while suppressing the excitation of WG-type modes. We fabricated samples with $M = 0.8$, 0.85, and 0.95. A scanning electron microscope image of a fabricated laser diode with $M = 0.95$ is shown in Fig. 4(a).

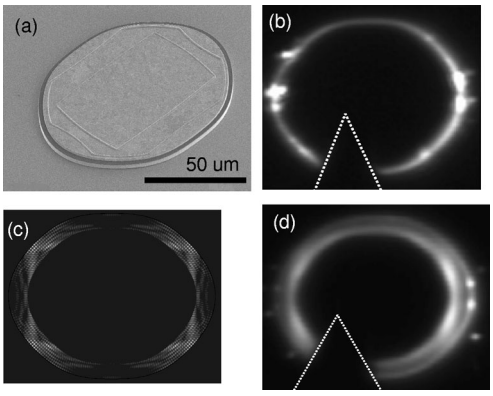

FIG. 4. (a) Scanning electron microscope image of a fabricated laser diode with the margin parameter $M = 0.95$ (see text). (b) CCD photo of a lasing diode with $M = 0.95$. (c) The wave function of a rectangle-orbit mode covered by the electrode metal area with $M = 0.8$. (d) CCD photo of a lasing diode with $M = 0.8$. In (b) and (d), the photo is taken from a slightly oblique angle and the shade of an electrode is indicated by dotted lines.

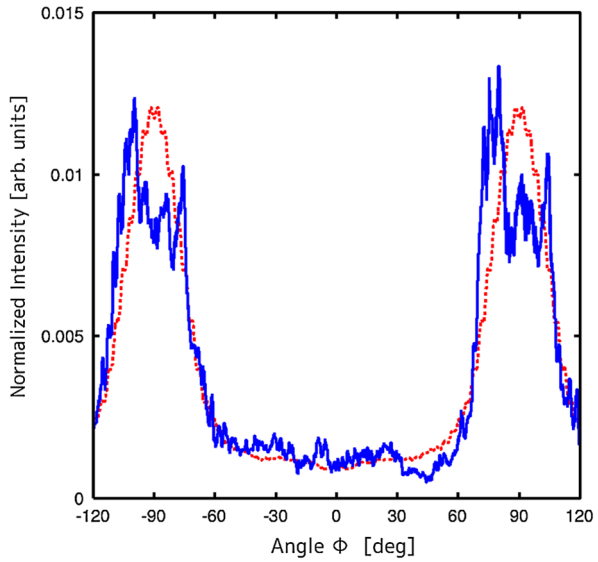

FIG. 5 (color online). Far-field emission patterns: experiment (solid curve) vs wave calculation (dotted curve). The experimental data are for a diode with the margin parameter $M = 0.95$. The numerical data are for the rectangle-orbit mode shown in Fig. 2, where rapid oscillation due to interference is smeared out.

We tested the laser diodes at 25 °C using a pulsed current of 500-ns width at 1-kHz repetition. Figure 5 shows a measured far-field pattern for the diode with $M = 0.95$ at the injection current 500 mA, together with a wave-calculated far-field pattern corresponding to the mode shown in Fig. 2. Both data are normalized so that integration becomes unity. Before the normalization of the experimental data, uniform background contribution due to spontaneous emission is subtracted so that the emission level around $\phi = 0$ coincides with that of the wave-calculated data. In Fig. 5, one can confirm excellent agreement between the experimental and calculated data. Far-field patterns for samples with $M = 0.8$ and 0.85 are found to be similar to that for $M = 0.95$, while substructures of the two main peaks are different. At the current strength 500 mA, we checked from an optical spectrum that lasing occurs in multimode. We expect that substructures of the main peaks observed in the experimental data are due to the effect of multimode lasing and thus depend on samples. Sample-specific details will be reported elsewhere.

In order to observe which positions of the cavity light is emitted from, we performed a near-field measurement of the cavity in lasing operation by using a CCD camera. The result is shown in Fig. 4(b) for a sample with $M = 0.95$, where we can observe scattered light at the cavity boundary. In good accordance with the numerical results, we can clearly observe that light is emitted from two points on each side of the cavity.

Figure 4(d) shows a near-field photo of a lasing diode with $M = 0.8$. The pattern observed in the margin area is considered to be formed by scattered light inside the cavity, reflecting the internal modal pattern. We show in Fig. 4(c) corresponding numerical data showing the wave function of a rectangle-orbit mode superimposed by the $M = 0.8$ electrode metal. Comparing these results, we find bright regions of the near-field photo corresponding to the left-arm and right-arm parts of the rectangle-orbit mode. This further convinces us the excitation of the rectangle-orbit modes.

In conclusion, we have demonstrated chaos-assisted directional light emission from the deformed disk semiconductor microcavity lasers. Theoretical analysis of resonant modes strongly localized along the TIR-confined rectangular orbit reveals that their directional emission, unexpected from the geometry of the rectangular orbit, can be fully explained by tunneling to chaotic orbits eventually escaping from the cavity following unstable manifolds around the critical line for TIR. In experiments, selectively exciting the rectangle-orbit modes, we succeeded in observing the chaos-assisted directional light emission in both the far and near fields, which provides decisive experimental evidence of dynamical tunneling in a ray-chaotic microcavity.

We would like to thank Jan Wiersig and Jung-Wan Ryu for discussions. S. S. and M. H. acknowledge financial support from the DFG research group 760 "Scattering Systems with Complex Dynamics" and the DFG Emmy Noether Program.

[1] L. Kelvin, Philos. Mag. Ser. 6, **2**, 1 (1901).
[2] H.-J. Stöckmann, *Quantum Chaos: An Introduction* (Cambridge University Press, Cambridge, U.K., 1999).
[3] J. U. Nöckel and A. D. Stone, Nature (London) **385**, 45 (1997).
[4] C. Gmachl *et al.*, Science **280**, 1556 (1998); S. B. Lee *et al.*, Phys. Rev. Lett. **88**, 033903 (2002); M. Lebental *et al.*, Appl. Phys. Lett. **88**, 031108 (2006); W. Fang *et al.*, Appl. Phys. Lett. **90**, 081108 (2007).
[5] T. Fukushima and T. Harayama, IEEE J. Sel. Top. Quantum Electron. **10**, 1039 (2004).
[6] For a review, see, for example, H. G. L. Schwefel *et al.*, in *Optical Microcavities*, edited by K. Vahala (World Scientific, Singapore, 2004).
[7] H. G. L. Schwefel *et al.*, J. Opt. Soc. Am. B **21**, 923 (2004); S.-Y. Lee *et al.*, Phys. Rev. A **72**, 061801(R) (2005); S. Shinohara *et al.*, Phys. Rev. A **74**, 033820 (2006); S.-B. Lee *et al.*, Phys. Rev. A **75**, 011802(R) (2007).
[8] J. Wiersig and M. Hentschel, Phys. Rev. Lett. **100**, 033901 (2008).
[9] M. J. Davis and E. J. Heller, J. Chem. Phys. **75**, 246 (1981).
[10] G. Hackenbroich and J. U. Nöckel, Europhys. Lett. **39**, 371 (1997); V. A. Podolskiy and E. E. Narimanov, Opt. Lett. **30**, 474 (2005); E. E. Narimanov and V. A. Podolskiy, IEEE J. Sel. Top. Quantum Electron. **12**, 40 (2006); A. Bäcker *et al.*, Phys. Rev. A **79**, 063804 (2009).
[11] H. E. Türeci *et al.*, Opt. Express **10**, 752 (2002).
[12] J. Wiersig, J. Opt. A **5**, 53 (2003).